Development 136, 2653-2663 (2009) doi:10.1242/dev.038430

Regulation of cell surface protease matriptase by HAI2 is essential for placental development, neural tube closure and embryonic survival in mice

Roman Szabo[1], John P. Hobson[1,*], Kristina Christoph[1], Peter Kosa[1], Karin List[2] and Thomas H. Bugge[1,†]

Hypomorphic mutations in the human *SPINT2* gene cause a broad spectrum of abnormalities in organogenesis, including organ and digit duplications, atresia, fistulas, hypertelorism, cleft palate and hamartoma. *SPINT2* encodes the transmembrane serine protease inhibitor HAI2 (placental bikunin), and the severe developmental effects of decreased HAI2 activity can be hypothesized to be a consequence of excess pericellular proteolytic activity. Indeed, we show here that HAI2 is a potent regulator of protease-guided cellular responses, including motogenic activity and transepithelial resistance of epithelial monolayers. Furthermore, we show that inhibition of the transmembrane serine protease matriptase (encoded by *St14*) is an essential function of HAI2 during tissue morphogenesis. Genetic inactivation of the mouse *Spint2* gene led to defects in neural tube closure, abnormal placental labyrinth development associated with loss of epithelial cell polarity, and embryonic demise. Developmental defects observed in HAI2-deficient mice were caused by unregulated matriptase activity, as both placental development and embryonic survival in HAI2-deficient embryos were completely restored by the simultaneous genetic inactivation of matriptase. However, neural tube defects were detected in HAI2-deficient mice even in the absence of matriptase, although at lower frequency, indicating that the inhibition of additional serine protease(s) by HAI2 is required to complete neural development. Finally, by genetic complementation analysis, we uncovered a unique and complex functional interaction between HAI2 and the related HAI1 in the regulation of matriptase activity during development. This study indicates that unregulated matriptase-dependent cell surface proteolysis can cause a diverse array of abnormalities in mammalian development.

KEY WORDS: Kunitz-type inhibitors, Embryonic development, Neural tube defects, Nonalleic noncomplementation, Placental labyrinth, Tissue morphogenesis, Mouse

INTRODUCTION

The several hundred proteases that reside within the extracellular and pericellular space in vertebrates are essential modulators of cell behavior in the context of development, tissue homeostasis and tissue remodeling. Chief functions of this large class of enzymes include pruning of the extracellular matrix, activation of hormones, growth factors and cytokines, and ectodomain shedding of cell surface receptors and adhesion molecules. A common feature of proteases is their synthesis as inactive zymogens that are activated by endoproteolytic cleavage within a highly conserved activation site. This activation step is irreversible, and the active proteases are then regulated by cognate macromolecular protease inhibitors that usually bind directly to the active site, thereby blocking proteolytic activity and frequently causing internalization and degradation of the protease-inhibitor complex (Herz and Strickland, 2001; Lopez-Otin and Bond, 2008; Page-McCaw et al., 2007; Puente et al., 2003; Rau et al., 2007).

A potentially dramatic illustration of the requirement for postactivation regulation of protease activity during tissue morphogenesis was given by the recent discovery that humans homozygous or compound heterozygous for an assortment of *SPINT2* mutations suffer from an exceptionally broad range of developmental abnormalities that include duplication of internal organs, duplication and abnormal location of digits, craniofacial dysmorphisms, anal and choanal atresia, fistulas and harmatoma. Defects in postnatal epithelial function, such as persistent sodium diarrhea, corneal erosions and abnormal hair, are also associated with *SPINT2* deficiency (Heinz-Erian et al., 2009). The *SPINT2* gene encodes a serine protease inhibitor, hepatocyte growth factor activator inhibitor (HAI) 2 (also known as placental bikunin; hereafter HAI2) (Kawaguchi et al., 1997; Marlor et al., 1997), and reduced expression of HAI2 or synthesis of HAI2 variants with reduced in vitro inhibitory activity is common to all the mutated *SPINT2* alleles (Heinz-Erian et al., 2009). This raises the possibility that key morphogenic processes, such as organ and digit specification and tubulogenesis, may require the fine-tuning of pericellular proteolytic activity through HAI2 silencing of unknown target proteases. Alternatively, HAI2, a transmembrane protein, could have signaling or cell adhesion functions that are independent of its protease inhibitory activity.

HAI2 is a Kunitz-type serine protease inhibitor named after its homology to hepatocyte growth factor activator inhibitor 1 and its first isolation from human placenta, respectively (Kawaguchi et al., 1997; Marlor et al., 1997). It is an integral type I transmembrane glycoprotein consisting of a short cytoplasmic tail, a single transmembrane domain and an extracellular tandem array of Kunitz inhibitory domains. The isolated Kunitz inhibitory domains of HAI2 display potent inhibitory activity towards more than a dozen trypsin-like serine proteases when tested in cell-free in vitro systems. These include both membrane serine proteases such as hepsin, matriptase and prostasin, as well as secreted proteases such as tissue kallikrein, plasma kallikrein, hepatocyte growth factor activator, and coagulation factors IXa, Xa, XIa and XIIa (Delaria et al., 1997;

[1]Oral and Pharyngeal Cancer Branch, National Institute of Dental and Craniofacial Research, National Institutes of Health, Bethesda, MD 20892, USA. [2]Department of Pharmacology, Barbara Ann Karmanos Cancer Institute, Wayne State University School of Medicine, Detroit, MI 48201, USA.

*Present address: Meso Scale Diagnostics, Gaithersburg, MD 20877, USA
†Author for correspondence (e-mail: thomas.bugge@nih.gov)

Accepted 4 June 2009

Herter et al., 2005; Kirchhofer et al., 2005; Qin et al., 1998; Szabo et al., 2008). This list of in vitro targets may be even larger, as HAI2 has been tested for inhibitory activity towards only a small fraction of the trypsin-like serine proteases encoded by the human genome. This suggests that inhibitory target selectivity by HAI2 is achieved primarily through temporal and spatial restrictions, such as the site of expression, membrane anchorage and subcellular localization, thus complicating the identification of key developmental and postnatal HAI2 targets using standard biochemical approaches. However, *SPINT2* orthologs are found in the genomes of all mammals analyzed, indicating a conserved function in development (Quesada et al., 2009), which makes target identification amenable to a combination of cell biological, genomic and genetic approaches, such as epistasis and complementation analysis in mice.

ST14 encodes the type II transmembrane serine protease, matriptase, that is expressed in many epithelial tissues and plays a crucial postnatal role in the terminal differentiation of the epidermis and other epithelial tissues in both humans and rodents (Alef et al., 2008; Basel-Vanagaite et al., 2007; List et al., 2006a; List et al., 2003). Previous studies by our group and by others have shown that dysregulation of matriptase in intact tissues by ectopic expression or loss of inhibition can perturb homeostasis by derailing proliferative and migratory cellular circuits (Carney et al., 2007; List et al., 2005; Mathias et al., 2007).

In this study, we show that HAI2 is a potent modulator of cell behavior that is governed by resident trypsin-like serine proteases. The use of transcriptomic profiling, combined with epistasis and complementation analysis, identified matriptase as a key target for HAI2 during tissue morphogenesis, and revealed a complex redundancy of HAI2 and the related HAI1 in matriptase regulation. This study establishes that tissue morphogenesis requires postactivation regulation of membrane-associated serine proteases by a network of partially redundant Kunitz-type transmembrane protease inhibitors.

MATERIALS AND METHODS

Cell culture

Type I and type II Madin-Darby canine kidney (MDCK) cells were kindly provided by Dr Jay Chiorini (NIDCR, Bethesda, MD, USA). The cells were maintained in Dulbecco's Modified Eagle Medium (DMEM) containing high glucose and supplemented with 10% fetal bovine serum, penicillin/streptomycin and 2 mM L-glutamine (all Gibco, Invitrogen, Carlsbad, CA, USA), and were cultured in a 5% CO_2-buffered tissue culture incubator. To generate cells with cytomegalovirus promoter-driven expression of full-length human HAI2 protein, the 1.3 kb *Eco*RI fragment of the pOTB7 vector containing the entire coding region of the human *SPINT2* cDNA (IMAGE clone 3952243, nucleotide –293 to +1035 of the *SPINT2* cDNA) was cloned into the mammalian expression plasmid pLenti-EF-1-SfiI-shuttle-IRES-PuroR (a kind gift from Drs Daniel Martin and Silvio Gutkind, NIDCR). MDCK type I cells were transfected with pLenti-EF-1-SfiI-shuttle-IRES-PuroR/hSpint2 or control pLenti-EF-1-SfiI-shuttle-IRES-PuroR plasmid DNA using PolyFect Reagent (Qiagen, Valencia, CA, USA) following the manufacturer's instructions. Transfected cells were selected by adding 5 μg/ml of puromycin (Sigma, St Louis, MO, USA) into the culturing medium, using untransfected cells as a negative control. Stably transfected HAI2-expressing and mock-transfected clones (several hundred) were each pooled and the expression of HAI2 was determined by western blot as described below.

Western blot

MDCK I cells stably transfected with HAI2-expressing plasmid or control plasmid were grown on 100 mm cell culture dishes to ~90% confluency, washed with PBS and lysed in buffer containing 62.5 mM Tris-HCl pH 6.8, 2% SDS and 10% glycerol, and subjected to a western blot analysis as described previously (Szabo et al., 2005). Anti-human HAI2 primary antibody (R&D Systems, Minneapolis, MN, USA) and anti-goat secondary antibodies (Sigma) conjugated with alkaline phosphatase were used.

Trans epithelial electric resistance (TEER) measurements/proliferation assays

MDCK type I cells (25,000 per well) expressing full-length human HAI2 or mock-transfected control cells (see above) were seeded in triplicate into 6.5 mm Transwell chambers (Corning, Lowell, MA, USA). The transepithelial ion permeability of monolayers was determined every 24 hours by measuring electric resistance across the epithelial monolayer using the EVOM Epithelial Voltohmmeter (World Precision Instruments, Saratosa, FL, USA). The medium in both internal and external compartments of each Transwell was changed every 2 days.

Cell motility assay

MDCK type II cells (5000 per well) were seeded into 12-well plates and allowed to form isolated colonies in serum-containing DMEM medium. Cells were then washed once with PBS and incubated in serum-free DMEM at 37°C for 1 hour. The medium was then replaced with serum-free DMEM containing 100 ng/ml of pro-HGF/SF or 100 ng/ml active HGF/SF (R&D Systems) and the soluble extracellular domain of human recombinant HAI2 protein (R&D Systems) was added to a final concentration of 0, 5, 20 or 60 nM. Aprotinin (1 μM) was added to cells as a positive control for the inhibition of pro-HGF/SF activation. The experiments were performed at least twice and in duplicates.

Cell proliferation assay

MDCK I cells stably transfected with a human HAI2 expression vector or an empty expression vector were seeded onto 60 mm plates (10,000 cells) and grown in serum-containing DMEM medium with high glucose. The number of cells in three separate areas of approximately 1 cm^2 each was counted every 24 hours for period of 7 days.

Cell apoptosis assay and determination of cell size

To determine the effect of HAI2 expression on the overall cell size and apoptotic rate of MDCK I cells during the acquisition of transepithelial electrical resistance (TEER), 4×10^5 MDCK I cells expressing full-length human recombinant HAI2 protein or MCDK I control cells were seeded in triplicate into 24 mm Transwell chambers and incubated in serum-containing DMEM medium. The transepithelial ion permeability of monolayers was measured every 24 hours as described above. At the onset of TEER acquisition (96 hours after seeding) and once the cells reached maximum TEER values (168 hours after seeding), the relative rate of apoptosis was determined by measuring caspase 3 activity using a Caspase 3 Fluorometric Assay (R&D Systems) following the manufacturer's instructions. To measure the relative size of the cells, cells grown in Transwell chambers for 96 and 168 hours were detached from the bottom of the chamber by the addition of 0.05% Trypsin-EDTA (Gibco), centrifuged for 4 minutes at 500 ***g***, and resuspended in PBS (Gibco) with 0.5% bovine serum albumin (Sigma). Cells of each sample (5×10^4-10×10^4) were then subjected to flow cytometry using forward light scatter on a BD FACS Calibur System (BD Biosciences, San Jose, CA, USA), and the relative size of cells in each sample was analyzed using CellQuest Pro 5.2 software (BD Biosciences).

Gene-targeted mice

All procedures involving live animals were performed in an Association for Assessment and Accreditation of Laboratory Animal Care International-accredited vivarium, following Institutional Guidelines and standard operating procedures. The generation of mice carrying β-galactosidase-tagged *Spint2*, *Spint1* null, *St14* null and β-galactosidase-tagged *St14* alleles has been described previously (List et al., 2002; List et al., 2006b; Mitchell et al., 2001; Szabo et al., 2008; Szabo et al., 2007). Mice were genotyped for the presence of the *Spint2* null allele by PCR using HAI2-geo51 (5′-ATCTGCAACCTCAAGCTAGC-3′) and HAI2-geo31 (5′-CAGAA-CCAGCAAACTGAAGG-3′) primers, and for the presence of the *Spint2* wild-type allele using HAI2-wt51 (5′-AACACATTTCACCACCATGC-3′) and HAI2-wt31 (5′-CCAGACTTTCCTAAGTGGG-3′) primers. PCR

screening for *Spint1* null, β-galactosidase-tagged *St14* and *St14* null alleles has been described previously (List et al., 2002; List et al., 2006b; Szabo et al., 2008). All mice used in this study were in a mixed 129/C57BL/6J/BlackSwiss genetic background. Inherent to the lethality of mice homozygous for *Spint2*, *Spint1* and *St14* null alleles, all studies were littermate-controlled.

Extraction of embryonic and perinatal tissues

Breeding females were checked for vaginal plugs in the morning and the day on which the plug was found was defined as the first day of pregnancy (E0.5). Pregnant females were euthanized in the mid-day at designated time points by CO_2 asphyxiation. Embryos were extracted by Cesarian section and the individual embryos and placentae were dissected and processed as described below. Visceral yolk sacs of individual embryos were washed twice in PBS, subjected to genomic DNA extraction and genotyped by PCR. Newborn pups were euthanized by CO_2 inhalation at 0°C. For histological analysis, the embryos and newborn pups were fixed for 24 hours in 4% paraformaldehyde (PFA) in PBS, processed into paraffin, sectioned into parallel sagittal- or cross-sections and stained with Hematoxylin and Eosin (H&E), or used for immunohistochemistry as described below.

RNA extraction and RT-PCR

The *Spint2*-deficient and *Spint2*-expressing littermate control embryos were isolated as described above. Total RNA was prepared by extraction in TRIzol reagent (Gibco, Carlsbad, CA, USA), as recommended by the manufacturer. First-strand cDNA synthesis was performed from 1 μg of total RNA using a RETROscript Kit (Ambion) and an oligo-dT primer according to the manufacturer's instructions. The subsequent PCR (denaturation temperature 92°C, annealing temperature 55°C, extension temperature 72°C, 35 cycles) was carried out using HAI2-RT51 (5′-CTGGCA-GCAGGTCATGG-3′) and HAI2-RT31 (5′-TTGCCATTGCCTTCAC-AGCC-3′) primers. To verify the identity of the RT-PCR products, the amplified DNA was excised from the agarose gel following electrophoresis, purified and analyzed by DNA sequencing.

Immunohistochemistry

Tissues were fixed overnight in 4% PFA, embedded in paraffin and cut into 5 μm-thick sections. Antigens were retrieved by incubation for 10 minutes at 37°C with 10 μg/ml proteinase K (Fermentas, Hanover, MD, USA) for HAI1 staining, or by incubation for 20 minutes at 100°C in 0.01 M sodium citrate buffer pH 6.0, for all other antigens. The sections were blocked with 2% bovine serum albumin in PBS and incubated overnight at 4°C with anti-laminin (Sigma), anti-CD31 (Santa Cruz Biotechnology, Santa Cruz, CA, USA), anti-HAI1 (R&D Systems), or anti-matriptase (R&D Systems) primary antibodies. Bound antibodies were visualized using biotin-conjugated anti-mouse, -rabbit, -sheep or -goat secondary antibodies (Vector Laboratories, Burlingame, CA, USA) and a Vectastain ABC Kit (Vector Laboratories), using 3,3′-diaminobenzidine as the substrate (Sigma). All microscopic images were acquired on a Olympus BX40 microscope using an Olympus DP70 digital camera system (Olympus, Melville, NY, USA).

Whole-mount β-galactosidase staining

Tissue samples were fixed for 30 minutes in 4% PFA in PBS, rinsed in PBS and stained with a β-galactosidase staining kit (Roche, Indianapolis, IN, USA) for 6 hours at 37°C using X-Gal as the substrate. The tissues were postfixed overnight in 4% PFA, embedded in paraffin, sectioned and stained with nuclear Fast Red. All analysis included parallel staining of wild-type littermate control mice to ensure the specificity of the staining.

Folate injections

Spint2 heterozygous females bred to *Spint2* heterozygous males were checked for vaginal plugs. Folic acid (10 mg/g body weight, Sigma) in PBS was administered to pregnant females by intraperitoneal injection every 24 hours starting on E0.5. Embryos were extracted on E10.5 by Cesarian section, genotyped as described above and scored for neural tube closure defects.

Transcriptomal analysis of trypsin-like serine proteases

The cranial region of the neural tube with adjacent surface epithelium was microdissected from wild-type E8.5 embryos. Total RNA was extracted from the dissected tissue and reverse-transcribed into cDNA as described above. PCR amplification was performed using the degenerate oligonucleotide primers mSPD52 [5′-GT(G/T)(C/G)T(G/T)-(A/T)C(A/T)GCTGC(A/T/C)CACTG-3′] and mSPD32 [5′-(A/T)GGGCC(A/T)CC(A/T/G)GAGTC(A/T)CC-3′], corresponding to the conserved amino acid sequences Val-Leu-Thr-Ala-Ala-His-Cys and Gly-Asp-Ser-Gly-Gly-Pro-Leu, respectively, as described previously (Takano et al., 2004). Fragments of 400-500 base pairs (bp) in size were recovered from the PCR products by agarose gel electrophoresis. The PCR products of the expected size of 400-500 bp were extracted from agarose gels following electrophoresis, subcloned into the TOPO TA vector (Invitrogen) and the identity of the inserted DNA was then determined by sequencing. A total of 600 plasmid-transformed bacterial clones with an identified PCR insert were screened.

RESULTS

HAI2 is a potent modulator of cell behavior initiated by the resident trypsin-like serine proteases

The potent and promiscuous activity of the Kunitz-type domains of HAI2 towards trypsin-like serine proteases suggests that *Spint2* supports development and maintains epithelial homeostasis by regulating the pericellular activity of one or more members of this large class of enzymes that regulates multiple cellular processes, including the bioavailability of growth factors, ion fluxes and paracellular permeability (Bhatt et al., 2007; Carattino et al., 2008; Chin et al., 2008; Cohen et al., 1985; Lee et al., 2000; Leyvraz et al., 2005; Mizuno et al., 1994; Myerburg et al., 2006; Naldini et al., 1992; Picard et al., 2008; Scudamore et al., 1998; Shimomura et al., 1993; Vallet et al., 1997; Wang et al., 1994a; Wang et al., 1996; Wang et al., 1994b). To survey the portfolio of biological activities that can be modulated by HAI2, we first manipulated the levels of the protease inhibitor either through overexpression or exogenous addition of a soluble bioactive version. For this purpose, we chose Madine-Darby canine kidney (MDCK) epithelial cells, as the aforementioned processes are regulated in a trypsin-like serine protease-dependent manner in this cell type. Exposure of MDCK type II cells to pro-hepatocyte growth factor/scatter factor (pro-HGF/SF) caused a well-described and conspicuous dissolution of cell-cell junctions of monolayers of cells and the subsequent migration of individual cells out of the cluster (Fig. 1A,B). Interestingly, this classic response was inhibited in a dose-dependent manner by the presence of nanomolar concentrations of the soluble extracellular domain of HAI2 (Fig. 1C,D; see Fig. S1A in the supplementary material). However, the scattering process proceeded normally in the presence of soluble HAI2 when cells were exposed to equimolar concentrations of proteolytically activated HGF/SF (Fig. 1E,F), showing that HAI2 might act on cell motility by regulating the bioavailability of HGF/SF at the level of its proteolytic conversion by endogenous MDCK-expressed trypsin-like serine proteases. MDCK type I cells, when unexposed to motility-inducing growth factors, form functional tight junctions whose ion permeability is modulated by proteolytic activity generated by trypsin-like serine proteases (Scudamore et al., 1998). To determine the potential effects of HAI2 levels on protease-modulated tight junction function, we measured the acquisition of transepithelial electrical resistance (TEER) in MDCK type I cells with increased expression of HAI2 (Fig. 1G). The proliferative capacity, outwards morphology, size

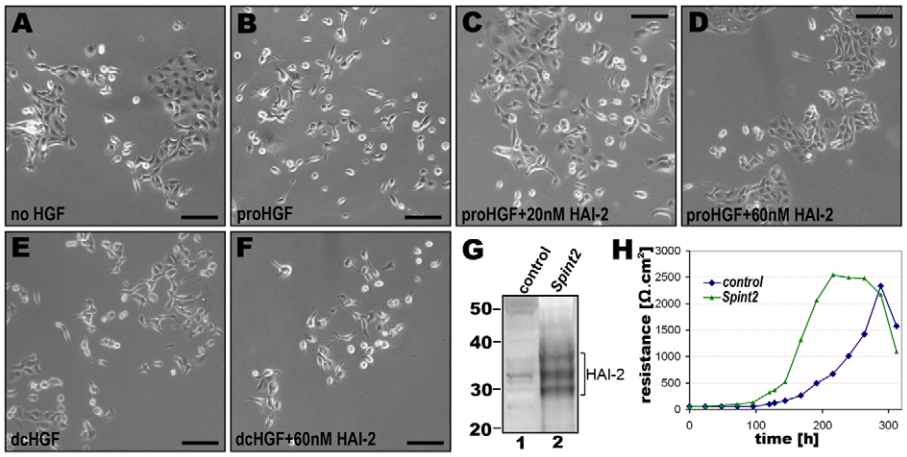

Fig. 1. HAI2 modulates epithelial cell behavior. (**A-F**) Inhibition of HGF/SF-induced scattering of MDCK type II cells by HAI2. MDCK cells were grown in serum-free medium in the absence of HGF/SF (A), or in the presence of 100 ng/ml of pro-HGF/SF (B-D) or active HGF/SF (E,F). Addition of 20 nM (C) or 60 nM (D,F) human recombinant HAI2 protein inhibited cell scattering induced by pro-HGF/SF (C,D), but not by active HGF/SF (F). (**G**,**H**) Increased expression of HAI2 accelerates acquisition of transepithelial resistance by MDCK type I cells. (G) Western blot analysis of HAI2 expression in MDCK type I cells stably transfected with a control vector (lane 1) and a *Spint2* expression vector (lane 2) shows strong expression of HAI2 protein in *Spint2*-transfected cells. (H) Measurement of transepithelial electric resistance (TEER) of MDCK type I cells transfected with control and *Spint2* expression plasmids shows marked acceleration of TEER acquisition in cells expressing HAI2 protein. Values represent average of triplicate determinations. Scale bars: 25 μm.

and rate of apoptosis of the cells were unaffected by the level of HAI2 (see Fig. S1B-F in the supplementary material; data not shown). However, MDCK type I cells with increased levels of HAI2 displayed a pronounced acceleration of the rate of acquisition of functional tight junctions, reaching a maximum TEER 72 hours earlier than control MDCK type I cells (Fig. 1H). Taken together, these studies reveal HAI2 as a modulator of the capacity of trypsin-like serine proteases to regulate basic cellular responses, such as cell motility and transepithelial barrier formation.

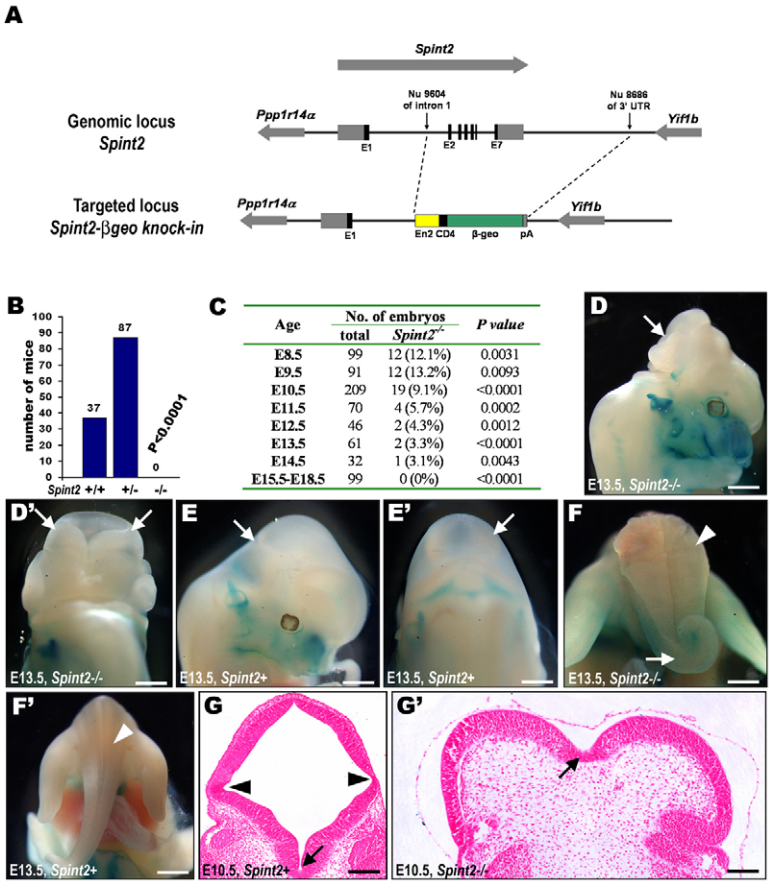

Fig. 2. HAI2 is essential for neural tube closure and embryonic survival. (**A**) Schematic representation of the β-galactosidase-encoding insertion into the mouse *Spint2* gene locus in the KST272 ES cell line. The targeting vector DNA that consists of the engrailed 2 (En2) splice acceptor site, CD4 transmembrane domain, β-galactosidase-encoding-neomycin phosphotransferase fusion gene (β-geo) and a bovine growth hormone polyadenylation site (pA) is inserted into intron 1 of the mouse *Spint2* gene. The insertion led to a deletion of an approximately 19 kb fragment of *Spint2* genomic DNA between nucleotide 9804 of intron 1 and nucleotide 8686 downstream of the stop codon of *Spint2* mRNA (vertical arrows). The deletion includes exons 2-7 of mouse *Spint2*, resulting in a *Spint2* null allele that produces a HAI2/β-geo fusion protein containing only the first 25 amino acid residues of murine HAI2 protein and, thus, is predicted to be devoid of any HAI2 inhibitory activity. (**B**) Distribution of genotypes of newborn mice from $Spint2^{+/-} \times Spint2^{+/-}$ breeding pairs. No $Spint2^{-/-}$ pups were detected. (**C**) Distribution of genotypes of embryos from $Spint2^{+/-} \times Spint2^{+/-}$ breeding pairs extracted by Cesarian section on E8.5-E18.5. About a half of the $Spint2^{-/-}$ embryos survive past E8.5 and no surviving $Spint2^{-/-}$ embryos were detected after E14.5. (**D-G'**) *Spint2* facilitates neural tube development. $Spint2^{-/-}$ embryos presented with exencephaly (D,D'; arrows), curly tail (F, arrow) and spina bifida (F, arrowhead). No neural tube defects were detected in $Spint2^{+/+}$ or $Spint2^{+/-}$ littermate embryos (E,E',F'). Histological analysis of neural tube closure in $Spint2^{+/+}$ (G) and $Spint2^{-/-}$ (G') embryos revealed that *Spint2* is dispensable for the formation of the medial hinge point (G,G'; arrow) but is required for the formation of dorsolateral hinge points (G, arrowheads). Scale bars: 200 μm in B-F'; 50 μm in G,G'.

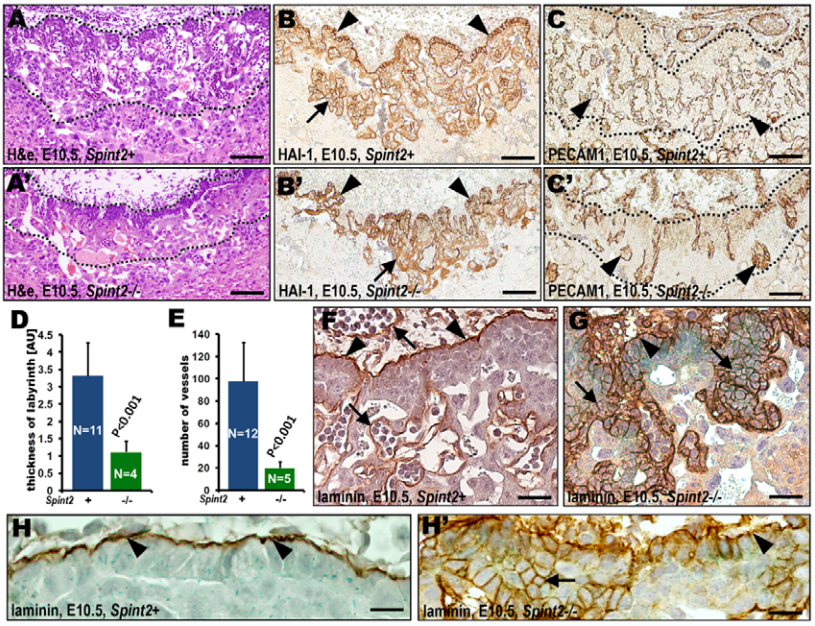

Fig. 3. *Spint2* facilitates placental branching morphogenesis. (**A**,**A′**) Representative histological (H&E) sections of *Spint2*-expressing (A) and *Spint2*-deficient (A′) placentae from E10.5 embryos showing placental labyrinth hypoplasia associated with loss of HAI2 (highlighted by dotted line). (**B-C′**) Visualization of chorionic and labyrinthine trophoblast cells by HAI1 staining (B,B′; arrowheads and arrows, respectively) and placental vascularization by staining for the endothelial cell marker PECAM1 (C,C′; arrowheads) in placentae from E10.5 *Spint2*$^{+}$ (B,C) and *Spint2*$^{-/-}$ (B′,C′) embryos. The staining shows decreased thickness and complexity of the labyrinth layer and fewer fetal vessels in *Spint2*$^{-/-}$ placentae. (**D**,**E**) Morphometric analysis of the thickness of the placental labyrinth (D) and the number of fetal vessels within the labyrinth (E) of *Spint2*$^{+}$ (blue) and *Spint2*$^{-/-}$ (green) E10.5 placentae. (**F-H′**) Expression of basement membrane marker laminin in E10.5 *Spint2*$^{+}$ (F,H) and *Spint2*$^{-/-}$ (G,H′) placentae. The staining shows structured deposition of laminin to the basement membrane at the basolateral surface of chorionic trophoblasts (F,H; arrowheads) and around the fetal endothelium (F, arrows) in *Spint2*-expressing placentae. However, deposition of laminin in *Spint2*-deficient placentae was frequently found around the entire periphery of chorionic trophoblasts (G,H′; arrows), showing loss of epithelial polarity. Scale bars: 75 μm in A-C′; 20 μm in F,G; 7.5 μm in H,H′.

Spint2 promotes placental branching morphogenesis and neural tube closure

We next used mouse reverse genetics to understand HAI2 function in the context of the developing embryo. In a preliminary phenotypic screen of a large array of randomly targeted mouse genes, homozygosity for a *lacZ*-tagged *Spint2* insertion was reported to result in embryonic lethality at gastrulation before embryonic day (E) 8, due to severe clefting of the embryonic ectoderm (Mitchell et al., 2001). Genomic analysis showed that the *lacZ* insertion was associated with the deletion of coding exons 2 through to 7, thus giving rise to a *Spint2* null allele (Fig. 2A). In agreement with the original analysis, our interbreeding of mice that were heterozygous for this *Spint2* allele (hereafter called *Spint2*$^{+/-}$) failed to produce any *Spint2*$^{-/-}$ pups among term offspring (Fig. 2B). However, mendelian analysis of multiple staged embryos showed that about half of the *Spint2*$^{-/-}$ embryos developed past E8 and proceeded to the headfold stage, although their survival decreased rapidly after E9.5, and none of the *Spint2*$^{-/-}$ embryos was found to live past E14.5 (Fig. 2C). Macroscopic inspection of *Spint2*$^{-/-}$ embryos that survived past E9.5 revealed severe defects in the development of the neural tube. Thus, 96% of *Spint2*$^{-/-}$ embryos extracted at E10.5 or later suffered from incomplete closure of the neural tube in the cranial region (exencephaly; Fig. 2D,D′), 89% of embryos extracted at E11.5 or later presented with a curly tail phenotype (Fig. 2F), indicative of a defect in secondary neurulation in the rostral region of the neural tube (Embury et al., 1979), and one *Spint2*$^{-/-}$ embryo suffered from an incomplete closure of the neural tube in the back region (spina bifida; Fig. 2F). None of the *Spint2*$^{+/+}$ or *Spint2*$^{+/-}$ mice was affected (Fig. 2E,E′,F′). These defects in neurulation were not rescued by the supplementation of dietary folate (data not shown). Whereas the genesis of the medial hinge of the developing neural tube appeared to proceed normally, the morphogenesis of the dorsolateral hinges of the neural epithelium was revealed to be *Spint2*-dependent (Fig. 2G,G′; data not shown).

Despite their severity, defects in neural tube closure are not known to abolish term development in either mice or humans (Kibar et al., 2007). However, careful macroscopic and histological inspection of *Spint2*$^{-/-}$ embryos did not reveal any additional morphological abnormalities in the embryo proper (data not shown), suggesting a possible additional requirement of *Spint2* for the development of extraembryonic tissues (yolk sac or placenta). Although no obvious effect of *Spint2* deficiency was observed on the outwards or histological appearance of the visceral yolk sac at E9.5 or E10.5 (data not shown), the development of the placental labyrinth was strongly impaired by homozygous *Spint2* deficiency (Fig. 3A,A′). Immunohistological staining for HAI1, a specific marker of chorionic and labyrinthine trophoblasts (Hallikas et al., 2006; Szabo et al., 2007) (Fig. 3B,B′), and CD31 (also known as PECAM), a marker for endothelial cells (Albelda et al., 1990) invading the labyrinth (Fig. 3C,C′), revealed a pronounced reduction in the thickness of the labyrinth (Fig. 3D) and a corresponding diminution of fetal vessel permeation of the labyrinthine space (Fig. 3E). Further analysis documented that most *Spint2*$^{-/-}$ placentae suffered from a pronounced defect in the polarization of the chorionic epithelium, as shown by delocalized deposition of the basement membrane protein laminin (Fig. 3F-H′). Placental abnormalities were not detected in *Spint2*$^{+/-}$

Table 1. Trypsin-like serine proteases expressed during neural tube formation

Protease	Gene name (Entrez Gene ID)	Number of hits
Secreted proteases		
Granzyme D and/or E*	*Gzmd* (14941) *Gzme* (14942)	110
Kallikrein-related peptidase 8	*Klk8* (259277)	95
Granzyme F	*Gzmf* (14943)	75
Tissue plasminogen activator	*Plat* (18791)	68
Kallikrein 1	*Klk1* (16612)	41
Kallikrein-related peptidase 7	*Klk7* (23993)	28
Granzyme C	*Gzmc* (14940)	15
Granzyme B	*Gzmb* (14939)	6
Chymotrypsin-like	*Ctrl* (109660)	3
Granzyme A	*Gzma* (14938)	1
Granzyme E and/or G†	*Gzme* (14942) *Gzmg* (14944)	1
Kallikrein-related peptidase 15	*Klk15* (317652)	1
Protease, serine, 12 (neurotrypsin, motopsin)	*Prss12* (19142)	1
Thrombin	*F2* (14061)	1
Membrane-bound proteases		
Prostasin	*Prss8* (76560)	53
Matriptase	*St14* (19143)	7
Matriptase3	*Tmprss7* (208171)	1
TMPRSS2	*Tmprss2* (50528)	1
TMPRSS4	*Tmprss4* (214523)	1

Nucleotide identity between granzyme D and E* and granzyme E and G† in the amplified region.

embryos at any stage, indicating that *Spint2* heterozygosity is permissive for normal placental development. These findings demonstrate that *Spint2* is essential to establish the functional maternal-fetal interface required for term development of the embryo, and that *Spint2*$^{-/-}$ embryos that succeed in clearing the first developmental hurdle prior to E8.0 succumb to oxygen and nutrient starvation at mid-gestation associated with placental failure.

Delineation of the trypsin-like serine protease transcriptome during *Spint2*-dependent morphogenesis

To identify potential HAI2 targets during morphogenesis, tissues from the cranial region of the developing neural tube of wild-type mice were isolated by microdissection and used for the generation of a cDNA library. Next, we used a previously devised strategy (Takano et al., 2004), which uses degenerate primers designed to be capable of amplifying trypsin-like serine proteases, to perform PCR amplification of the cDNA library and DNA sequencing of the ensuing amplicons. This analysis revealed the expression of genes encoding 17-19 different secreted or membrane-bound trypsin-like serine proteases during neurogenesis (Table 1). In addition to a number of genes encoding granzymes, these included genes encoding proteases known to be expressed in the developing central nervous system, such as tissue-type plasminogen activator, kallikrein-related protease 8 (neuropsin) and PRSS12 (neurotrypsin), and also the transmembrane serine proteases TMPRSS2, TMPRSS4, matriptase and matriptase 3, as well as the GPI-anchored protease prostasin. Notably, two of these transmembrane serine proteases, matriptase and prostasin, were recently reported to be efficiently inhibited by HAI2 in vitro and, thus, represented potential HAI2 targets during neural tube closure (Coote et al., 2009; Szabo et al., 2008) (see below).

Spint2 acts in situ to facilitate morphogenesis

To gain additional mechanistic insights into *Spint2*-dependent neural tube closure and placental branching morphogenesis, we took advantage of the insertion of the promoterless *lacZ* marker gene, encoding β-galactosidase, in the *Spint2* null allele (Fig. 2A) to determine the localization of *Spint2* expression in the two developmental processes by X-Gal staining of embryos carrying one wild-type and one *lacZ*-targeted allele. This analysis revealed a spatial and temporal correlation between neural and placental morphogenesis and the expression of *Spint2*, consistent with the notion that HAI2 is acting in the local pericellular microenvironment to facilitate development. Thus, *Spint2* expression was abundant in the developing neuroepithelium of the cranial region of the embryo, as well as at the caudal extremity of the embryo that develops in the tail region, at least as early as E7.5 and persisting until E9.5 (Fig. 4A-D; data not shown), thereby spanning the critical developmental window in which neural tube closure occurs (Kaufmann and Bart, 1999). Furthermore, histological analysis revealed that *Spint2* is expressed in cells at the point of contact between the two sides of the neural epithelium before neural tube closure occurs (Fig. 4E). Likewise, suggesting a localized mode of action in placental formation, *Spint2* was expressed specifically in chorionic trophoblasts and in the underlying trophoblast cells within the labyrinth, commencing as early as E8.0 and persisting for the duration of placental labyrinth development (Fig. 4F-H; data not shown).

Epistasis analysis identifies matriptase as a key morphogenic target for *Spint2*

One protease of particular interest that was identified in the transcriptomic analysis was matriptase, encoded by the *St14* gene. First, microarray analysis has shown that matriptase is expressed in MDCK cells (Hellman et al., 2008). Second, matriptase can proteolytically process and activate pro-HGF and the epithelial permeability-inducing PAR2 (F2RL1) (Lee et al., 2000; Takeuchi et al., 2000). Third, in addition to its expression in the developing neural tube, we have previously shown that matriptase is also expressed in chorionic trophoblasts during branching morphogenesis (Szabo et al., 2007). Fourth, soluble HAI2 displays potent inhibitory activity towards endogenous matriptase located on the surface of the monocytoid cell line THP-1 (Kilpatrick et al., 2006; Szabo et al.,

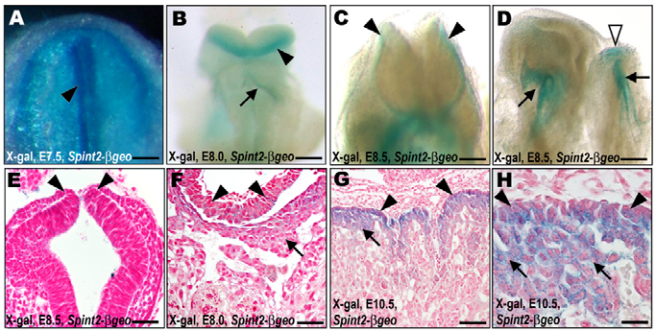

Fig. 4. *Spint2* is expressed in the developing neural tube and placenta. (**A-D**) Macroscopic appearance of E7.5 (A), E8.0 (B) and E8.5 (C,D) *Spint2-β-geo* knock-in embryos after X-Gal staining. *Spint2* expression was diffusely distributed throughout the embryo at E7.5, with the highest levels detected in the forming neural folds (A, arrowhead). At E8.0 and E8.5, the expression of *Spint2* was confined to the border between the neural and non-neural ectoderm in the head region of the embryo (B,C; arrowheads), and to the epithelium lining the foregut and hindgut diverticulum (B,D; arrows). At E8.5, *Spint2* expression was also detected at the caudal extremity of the embryo (future tail region; D; open arrowhead) (**E**) Histological analysis of *Spint2* expression in the developing neural tube in E8.5 *Spint2-β-geo* knock-in embryos. The expression was localized in the cells of both neural and non-neural ectoderm proximal to the region of neural tube closure (blue staining, arrowheads). (**F-H**) Histological analysis of the expression of *Spint2* in placentae of E8.5 (F) and E10.5 (G,H) *Spint2-β-geo* knock-in embryos. *Spint2* is located in chorionic trophoblasts (F-H, arrowheads) and in the underlying trophoblast cells within the labyrinth (F-H, arrows). Scale bars: 50 μm in A; 100 μm in B-D; 20 μm in E,F; 75 μm in G; 10 μm in H.

2008). To directly query the specific contribution of matriptase suppression by HAI2 to embryonic development, we took advantage of the availability of mice carrying an *St14* null allele, and the fact that *St14* by itself is dispensable for mouse term development (List et al., 2002). Our rationale was that if HAI2 suppression of matriptase was crucial for embryonic development, then the genetic ablation of *St14* should eliminate one or more of the developmental defects associated with *Spint2* deficiency. To test this hypothesis, we first bred $Spint2^{+/-}$ mice to $St14^{+/-}$ mice, and next interbred the ensuing $Spint2^{+/-};St14^{+/-}$ double-heterozygous mice to generate offspring carrying one or two wild-type *Spint2* and one or two wild-type *St14* alleles (hereafter termed $Spint2^{+};St14^{+}$), two *Spint2* null alleles and one or two *St14* wild-type alleles (hereafter termed $Spint2^{-/-};St14^{+}$), one or two *Spint2* wild-type alleles and two *St14* null alleles (hereafter termed $Spint2^{+};St14^{-/-}$), and two *Spint2* null alleles and two *St14* null alleles (hereafter termed $Spint2^{-/-};St14^{-/-}$). In agreement with data presented above, no $Spint2^{-/-};St14^{+}$ mice were identified among 226 term offspring from these crosses (Fig. 5A). Surprisingly, however, $Spint2^{-/-};St14^{-/-}$ pups were found in the expected mendelian frequency in the term offspring from the $Spint2^{+/-};St14^{+/-}$ double-heterozygous crosses (Fig. 5A). This demonstrates that both the early (pre-E8.0) demise that befalls about half of the *Spint2* null embryos and the mid-gestation lethality of the remaining *Spint2* null embryos were dependent on *St14* activity.

St14 elimination restores *Spint2* null placental development

We next extracted embryos with single and combined loss of *Spint2* and *St14* at different embryonic stages to directly determine the effect of *St14* ablation on the morphogenesis of *Spint2*-dependent tissues. Consistent with the re-establishment of term development, histological analysis of placental tissues from $Spint2^{-/-};St14^{-/-}$ embryos showed normal development of the placental labyrinth, as evidenced by both the restored thickness of the labyrinth layer (Fig. 5B,C; compare with Fig. 3B,B′), normal branching of fetal vessels into the labyrinthine layer (Fig. 5D,E; compare with Fig. 3C,C′) and the normal deposition of laminin by chorionic epithelial cells (Fig. 5F; compare with Fig. 3F,G). In agreement with our previous study (Szabo et al., 2007), *St14* expression could be detected specifically in chorionic trophoblasts

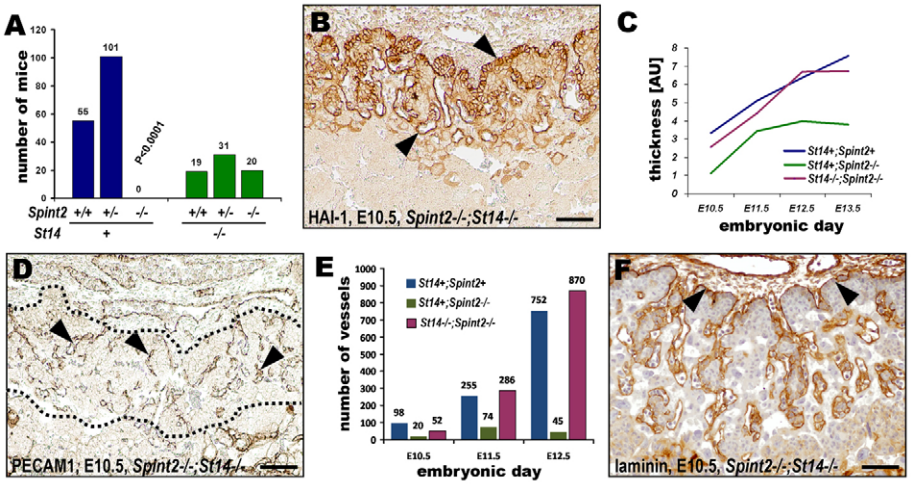

Fig. 5. *Spint2* genetically interacts with *St14*, which encodes matriptase. (**A**) Distribution of genotypes of newborn mice from $Spint2^{+/-};St14^{+/-} \times Spint2^{+/-};St14^{+/-}$ breeding pairs. Although no *St14*-expressing, $Spint2^{-/-}$ pups were detected, $Spint2^{-/-};St14^{-/-}$ mice were born in the expected mendelian ratio. (**B**,**C**) Histological staining for the placental labyrinth marker HAI1 (B, arrowheads) in E10.5 placenta and statistical analysis of the thickness of the placental labyrinth at E10.5-E13.5 (C) show restored trophoblast differentiation in $Spint2^{-/-};St14^{-/-}$ embryos. (**D**,**E**) Histological staining for the endothelial cell marker PECAM1 (D, arrowheads) in E10.5 placenta and statistical analysis of the number of fetal vessels within the placental labyrinth at E10.5-E12.5 (E) show restored complexity of the maternal-fetal blood interface in $Spint2^{-/-};St14^{-/-}$ embryos. (**F**) Histological staining shows normal deposition of laminin in the developing basement membrane (arrowheads) in $Spint2^{-/-};St14^{-/-}$ placentae. Scale bars: 75 μm.

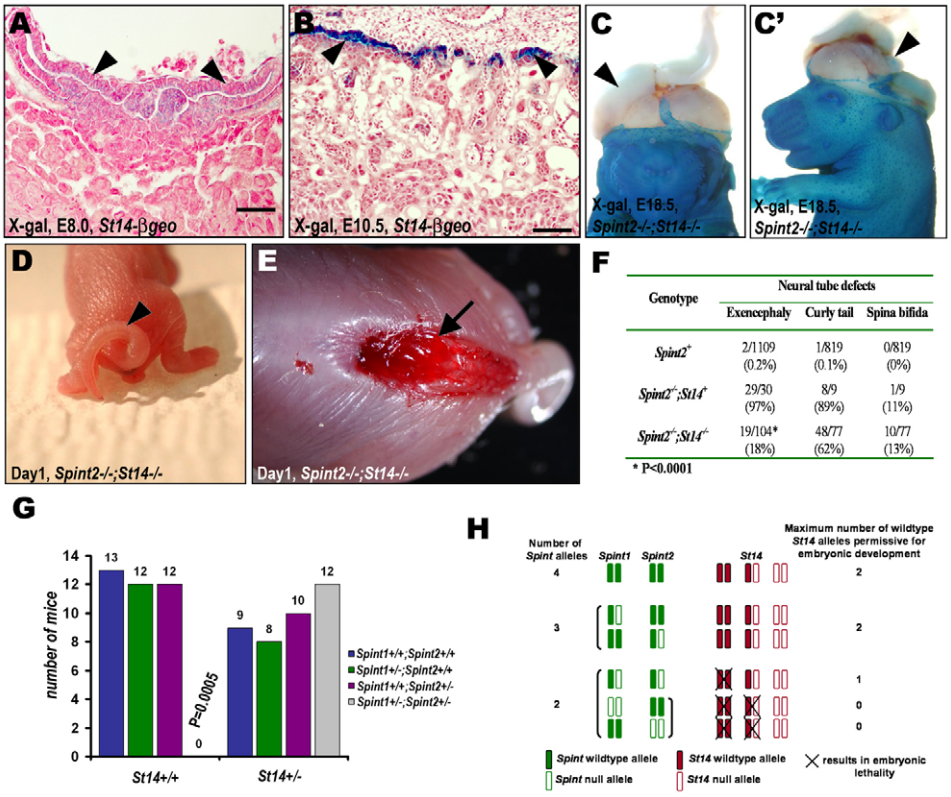

Fig. 6. Neural tube closure and embryonic survival in mice are regulated by a complex interaction between *Spint1*, *Spint2* and *St14*. (**A**,**B**) Histological analysis of *St14* expression in placentae extracted from E8.5 (A) and E10.5 (B) *St14-β-geo* knock-in embryos. *St14* is detected specifically in the chorionic trophoblasts (arrowheads). (**C-E**) Examples of neural tube defects in term *Spint2*$^{-/-}$;*St14*$^{-/-}$ offspring: exencephaly (C,C′; arrowheads); curly tail (D, arrowhead); and spina bifida (E, arrow). (**F**) Statistical analysis of the frequency of neural tube defects in *Spint2*$^{-/-}$;*St14*$^{-/-}$ embryos and newborn mice. Inactivation of *St14* dramatically decreased the proportion of animals with exencephaly, although it had little or no impact on the frequency of curly tail and spina bifida. (**G**) Distribution of genotypes of newborn mice from *Spint2*$^{+/-}$;*Spint1*$^{+/+}$;*St14*$^{+/-}$ mice crossed to *Spint2*$^{+/+}$;*Spint1*$^{+/-}$;*St14*$^{+/+}$ mice (see key). No *Spint1*$^{+/-}$;*Spint2*$^{+/-}$ pups with two functional *St14* alleles (*St14*$^{+/+}$) were detected. However, *Spint1*$^{+/-}$;*Spint2*$^{+/-}$ mice possessing only one functional *St14* allele (*St14*$^{+/-}$) were born in the expected ratio. (**H**) Schematic representation of the observed genetic interaction between *Spint1*, *Spint2* and *St14* genes during mouse embryonic development. Only animals with three or four functional alleles of *Spint1* or *Spint2* genes can tolerate two *St14* wild-type alleles during embryonic development. Mice with two functional *Spint1* or *Spint2* alleles do not survive in the presence of two functional alleles of *St14*, but can tolerate *St14* heterozygosity if they express both *Spint1* and *Spint2* (*Spint1*$^{+/-}$;*Spint2*$^{+/-}$ mice). Finally, if either of the Spint genes are completely inactivated (*Spint1*$^{-/-}$;*Spint2*$^{+/+}$ or *Spint1*$^{+/+}$;*Spint2*$^{-/-}$ mice), the animals can complete embryonic development only in the absence of *St14*, i.e. on a *St14*$^{-/-}$ background. Scale bars: 20 μm in A; 75 μm in B.

as early as E8.0 and colocalized with *Spint2* for the duration of labyrinth development, from E8.5 through to E11.5 (Fig. 6A,B; data not shown; compare with Fig. 4F,G). These data show that a local matriptase-dependent proteolytic pathway is the only essential target for inhibition by HAI2 during placental branching morphogenesis, and identifies an excess of matriptase activity by chorionic trophoblasts as the underlying cause of placental defects in *Spint2*-deficient embryos.

Matriptase is a crucial but not exclusive HAI2 inhibitory target during neural tube morphogenesis

Analysis of the macroscopic appearance of pre-term embryos and newborn *Spint2*$^{-/-}$;*St14*$^{-/-}$ mice revealed that the overall frequency of neural tube closure-related defects presenting as exencephaly (Fig. 6C,C′; data not shown) was reduced more than fivefold in *Spint2*$^{-/-}$;*St14*$^{-/-}$ offspring, compared with their *Spint2*$^{-/-}$;*St14*$^{+}$ siblings (Fig. 6F). Caudal neural tube development in *Spint2*-deficient embryos was less affected by the ablation of *St14*, with a 30% reduction in neural tube defects presenting as curly tail (Fig. 6D,F; data not shown) and no appreciable effect on the frequency of spina bifida (Fig. 6E,F). This indicates that the inhibition of a matriptase-dependent proteolytic pathway is one crucial molecular function of HAI2 in neural tube development. In contrast to placental development, however, the elimination of *St14* does not restore normal neural tube formation of all *Spint2* null embryos, indicating that HAI2 suppression of additional protease targets, besides matriptase, is functionally relevant to the processes of neurulation.

Complex interaction of *Spint2* and *Spint1* in developmental suppression of *St14*

The requirement of functional alleles of both *Spint2* (this study) and *Spint1* (Szabo et al., 2007) for the developmental suppression of *St14* during placental morphogenesis is counterintuitive in light of the high structural homology of the protease inhibitors encoded by the two genes, and their conspicuous colocalization in developing placental tissues. To investigate this apparent paradox, we took advantage of the localization of *Spint2*, *Spint1* and *St14* on separate chromosomes (7, 2 and 11, respectively) and, thus, their independent segregation, to

perform a combined complementation and epistasis analysis to determine their interrelationship. Unexpectedly, this study demonstrated that the combined heterozygosity of *Spint2* and *Spint1* was incompatible with term development. Thus, no *Spint2*$^{+/-}$;*Spint1*$^{+/-}$;*St14*$^{+/+}$ pups were identified in 76 offspring from crosses of *Spint2*$^{+/-}$;*Spint1*$^{+/+}$;*St14*$^{+/-}$ mice with *Spint2*$^{+/+}$;*Spint1*$^{+/-}$;*St14*$^{+/+}$ mice (Fig. 6G). This unusual outcome, which is termed nonallelic noncomplementation, has been described previously in mice, *Drosophila*, *C. elegans* and yeast (e.g. Hays et al., 1989; Rancourt et al., 1995; Rine and Herskowitz, 1987; Varkey et al., 1993). It shows that the expression of any three of the combined four *Spint1* and *2* alleles provides sufficient proteolytic inhibitory activity for term development, whereas the expression of any two of the four is insufficient. Even more informatively, this combined heterozygosity of *Spint2* and *Spint1* became permissive for term development once *St14* expression was reduced by the elimination of one functional *St14* allele. Indeed, *Spint1*$^{+/-}$;*Spint2*$^{+/-}$;*St14*$^{+/-}$ siblings were found at the expected frequency in term offspring from these crosses (Fig. 6G) and were outwardly normal (data not shown). Taken together (Fig. 6H), this analysis demonstrates that a delicate balance of the activity of the transmembrane serine protease matriptase and the inhibitory activities of HAI1 and HAI2 establishes a local pericellular proteolytic microenvironment that is conducive to successful tissue morphogenesis.

DISCUSSION

The current study shows that the pericellular availability of HAI2 is a potent determinant of protease-guided activities of cultured epithelial cells, including migratory responses and the acquisition of a diffusion barrier of confluent epithelial cell monolayers. The study also shows that focal inhibition of proteolytic activity by HAI2 is essential for fundamental developmental processes, such as branching morphogenesis and neural tube closure, and specifically identifies matriptase-dependent proteolysis as one crucial HAI2 target. Furthermore, our epistasis and complementation analysis revealed that a delicate balance of proteolytic activity, provided by matriptase and other serine protease(s), and serine protease inhibitory activity, provided by HAI2 and HAI1, creates a pericellular microenvironment that is permissive for the completion of these morphogenic processes. Thus, whereas *Spint2* null embryos failed to develop a functional labyrinth, form a neural tube and develop to term, the imposition of a simultaneous *St14* deficiency enabled placental development, greatly reduced the incidence of neural tube closure defects and enabled development to term. Additionally, combined heterozygosity for *Spint2* and *Spint1* was incompatible with development to term, whereas triple heterozygosity for *Spint2*, *Spint1* and *St14* enabled term development and postnatal survival. We propose that HAI2 acts by modulating protease-dependent migratory and homeostatic circuits in developing tissues by regulating the focal activity of matriptase and other trypsin-like serine proteases. In this regard, it is somewhat surprising that matriptase itself is dispensable for term development in humans, mice and zebrafish (Basel-Vanagaite et al., 2007; Carney et al., 2007; List et al., 2002). However, matriptase is one of three closely related proteases (Hooper et al., 2003; Szabo et al., 2005; Velasco et al., 2002). Moreover, matriptase 2 (TMPRSS6) and matriptase 3 display some overlap with matriptase in the pattern of expression during embryonic development (Hooper et al., 2003) (this study, and R.S. and T.H.B., unpublished data). It is therefore plausible that one or more of the three matriptases have redundant functions during development and that single deficiency in each is compatible with term development due to the compensatory activity of the others. Studies to experimentally test this hypothesis have been initiated.

The residual neural tube defects in combined *Spint2;St14* null mice reveal that neural tube closure is facilitated by HAI2 suppression of at least one additional protease besides matriptase. Our targeted transcriptomic analysis of the trypsin-like serine protease complement expressed during this morphogenic process revealed several potential candidates. Most notable among the additional 16-18 trypsin-like proteases expressed in the developing neural tube were the close matriptase relative, matriptase 3 (Szabo et al., 2005) and the type II transmembrane serine proteases TMPRSS2 (Paoloni-Giacobino et al., 1997) and TMPRSS4 (Wallrapp et al., 2000). Because the HAI2 Kunitz-type inhibitor domains are highly promiscuous in purified systems (see Introduction), the definitive identification of the residual morphogenic HAI2 targets will probably require exhaustive genetic complementation analysis.

Matriptase is an autoactivating protease that has been proposed to serve as an initiator of proteolytic cascades in adult tissues (Kilpatrick et al., 2006; Lee et al., 2000; Netzel-Arnett et al., 2006; Takeuchi et al., 2000). It is formally possible that HAI2 and HAI1 therefore do not target matriptase directly during development, but rather target proteases that are located downstream of matriptase. However, the potent inhibitory activity of HAI1 and HAI2 Kunitz-type inhibitory domains towards matriptase in vitro (Lin et al., 1999; Szabo et al., 2008) and the developmental colocalization of the two protease inhibitors with matriptase make this scenario unlikely.

The developmental consequences of *Spint2* deficiency at a superficial glance appear to manifest at an earlier stage in mice than humans and seem to be more severe. Importantly, however, to date, the known complement of mutated *SPINT2* alleles all either directed the production of HAI2 proteins at lower levels or with lower inhibitory activity (Heinz-Erian et al., 2009), whereas the phenotypic consequence of complete *Spint2* deficiency has been analyzed only in mice. Also, as only *SPINT2*-deficient individuals that completed term development have been available for clinical evaluation, it is premature to discuss potential species-specific variations in the developmental manifestations of the loss of HAI2. In addition to abnormal morphogenesis, HAI2 deficiency in humans is associated with distinct defects in postnatal epithelial homeostasis, as shown by severe corneal erosions, abnormal hair, persistent sodium diarrhea and poor postnatal survival. The abundant expression of matriptase in the epithelial compartment of all of these tissues (List et al., 2006b; Oberst et al., 2003) is a conspicuous indication that these postnatal manifestations might also be causally related to the loss of matriptase inhibition in these tissues.

In summary, this study establishes that a network of partially redundant Kunitz-type transmembrane protease inhibitors enables tissue morphogenesis through the local postactivation regulation of membrane-associated serine proteases.

Acknowledgements

Supported by the NIDCR Intramural Research Program of the NIH (T.H.B.) and by startup funds from Wayne State University (K.L.). We thank Dr Daniel Martin for the eukaryotic expression vector; Dr Jay Chiorini for MDCK cells; Dr Alfredo Molinolo for expert pathology support; Dr Joanne Konkel for valuable assistance with flow cytometry; and Drs J. Silvio Gutkind, Ken Yamada and Mary Jo Danton for critically reviewing this manuscript. Deposited in PMC for release after 12 months.

Supplementary material

Supplementary material for this article is available at http://dev.biologists.org/cgi/content/full/136/15/2653/DC1

References

Albelda, S. M., Oliver, P. D., Romer, L. H. and Buck, C. A. (1990). EndoCAM: a novel endothelial cell-cell adhesion molecule. *J. Cell Biol.* **110**, 1227-1237.

Alef, T., Torres, S., Hausser, I., Metze, D., Tursen, U., Lestringant, G. G. and Hennies, H. C. (2008). Ichthyosis, follicular atrophoderma, and hypotrichosis caused by mutations in ST14 is associated with impaired profilaggrin processing. *J. Invest. Dermatol.* **129**, 862-869.

Basel-Vanagaite, L., Attia, R., Ishida-Yamamoto, A., Rainshtein, L., Ben Amitai, D., Lurie, R., Pasmanik-Chor, M., Indelman, M., Zvulunov, A., Saban, S. et al. (2007). Autosomal recessive ichthyosis with hypotrichosis caused by a mutation in ST14, encoding type II transmembrane serine protease matriptase. *Am. J. Hum. Genet.* **80**, 467-477.

Bhatt, A. S., Welm, A., Farady, C. J., Vasquez, M., Wilson, K. and Craik, C. S. (2007). Coordinate expression and functional profiling identify an extracellular proteolytic signaling pathway. *Proc. Natl. Acad. Sci. USA* **104**, 5771-5776.

Carattino, M. D., Hughey, R. P. and Kleyman, T. R. (2008). Proteolytic processing of the epithelial sodium channel gamma subunit has a dominant role in channel activation. *J. Biol. Chem.* **283**, 25290-25295.

Carney, T. J., von der Hardt, S., Sonntag, C., Amsterdam, A., Topczewski, J., Hopkins, N. and Hammerschmidt, M. (2007). Inactivation of serine protease Matriptase1a by its inhibitor Hai1 is required for epithelial integrity of the zebrafish epidermis. *Development* **134**, 3461-3471.

Chin, A. C., Lee, W. Y., Nusrat, A., Vergnolle, N. and Parkos, C. A. (2008). Neutrophil-mediated activation of epithelial protease-activated receptors-1 and -2 regulates barrier function and transepithelial migration. *J. Immunol.* **181**, 5702-5710.

Cohen, E., Talmon, A., Faff, O., Bacher, A. and Ben-Shaul, Y. (1985). Formation of tight junctions in epithelial cells. I. Induction by proteases in a human colon carcinoma cell line. *Exp. Cell Res.* **156**, 103-116.

Coote, K., Atherton-Watson, H. C., Sugar, R., Young, A., MacKenzie-Beevor, A., Gosling, M., Bhalay, G., Bloomfield, G., Dunstan, A., Bridges, R. J. et al. (2009). Camostat attenuates airway epithelial sodium channel function *in vivo* through the inhibition of a channel-activating protease. *J. Pharmacol. Exp. Ther.* **329**, 764-774.

Delaria, K. A., Muller, D. K., Marlor, C. W., Brown, J. E., Das, R. C., Roczniak, S. O. and Tamburini, P. P. (1997). Characterization of placental bikunin, a novel human serine protease inhibitor. *J. Biol. Chem.* **272**, 12209-12214.

Embury, S., Seller, M. J., Adinolfi, M. and Polani, P. E. (1979). Neural tube defects in curly-tail mice. I. Incidence, expression and similarity to the human condition. *Proc. R. Soc. Lond. B Biol. Sci.* **206**, 85-94.

Hallikas, O. K., Aaltonen, J. M., von Koskull, H., Lindberg, L. A., Valmu, L., Kalkkinen, N., Wahlstrom, T., Kataoka, H., Andersson, L., Lindholm, D. et al. (2006). Identification of antibodies against HAI-1 and integrin alpha6beta4 as immunohistochemical markers of human villous cytotrophoblast. *J. Histochem. Cytochem.* **54**, 745-752.

Hays, T. S., Deuring, R., Robertson, B., Prout, M. and Fuller, M. T. (1989). Interacting proteins identified by genetic interactions: a missense mutation in alpha-tubulin fails to complement alleles of the testis-specific beta-tubulin gene of Drosophila melanogaster. *Mol. Cell. Biol.* **9**, 875-884.

Heinz-Erian, P., Muller, T., Krabichler, B., Schranz, M., Becker, C., Ruschendorf, F., Nurnberg, P., Rossier, B., Vujic, M., Booth, I. W. et al. (2009). Mutations in SPINT2 cause a syndromic form of congenital sodium diarrhea. *Am. J. Hum. Genet.* **84**, 188-196.

Hellman, N. E., Spector, J., Robinson, J., Zuo, X., Saunier, S., Antignac, C., Tobias, J. W. and Lipschutz, J. H. (2008). Matrix metalloproteinase 13 (MMP13) and tissue inhibitor of matrix metalloproteinase 1 (TIMP1), regulated by the MAPK pathway, are both necessary for Madin-Darby canine kidney tubulogenesis. *J. Biol. Chem.* **283**, 4272-4282.

Herter, S., Piper, D. E., Aaron, W., Gabriele, T., Cutler, G., Cao, P., Bhatt, A. S., Choe, Y., Craik, C. S., Walker, N. et al. (2005). Hepatocyte growth factor is a preferred *in vitro* substrate for human hepsin, a membrane-anchored serine protease implicated in prostate and ovarian cancers. *Biochem. J.* **390**, 125-136.

Herz, J. and Strickland, D. K. (2001). LRP: a multifunctional scavenger and signaling receptor. *J. Clin. Invest.* **108**, 779-784.

Hooper, J. D., Campagnolo, L., Goodarzi, G., Truong, T. N., Stuhlmann, H. and Quigley, J. P. (2003). Mouse matriptase-2: identification, characterization and comparative mRNA expression analysis with mouse hepsin in adult and embryonic tissues. *Biochem. J.* **373**, 689-702.

Kaufmann, M. H. and Bart, S. (1999). *The Anatomical Basis of Mouse Development*. San Diego, CA: Academic Press.

Kawaguchi, T., Qin, L., Shimomura, T., Kondo, J., Matsumoto, K., Denda, K. and Kitamura, N. (1997). Purification and cloning of hepatocyte growth factor activator inhibitor type 2, a Kunitz-type serine protease inhibitor. *J. Biol. Chem.* **272**, 27558-27564.

Kibar, Z., Capra, V. and Gros, P. (2007). Toward understanding the genetic basis of neural tube defects. *Clin. Genet.* **71**, 295-310.

Kilpatrick, L. M., Harris, R. L., Owen, K. A., Bass, R., Ghorayeb, C., Bar-Or, A. and Ellis, V. (2006). Initiation of plasminogen activation on the surface of monocytes expressing the type II transmembrane serine protease matriptase. *Blood* **108**, 2616-2623.

Kirchhofer, D., Peek, M., Lipari, M. T., Billeci, K., Fan, B. and Moran, P. (2005). Hepsin activates pro-hepatocyte growth factor and is inhibited by hepatocyte growth factor activator inhibitor-1B (HAI-1B) and HAI-2. *FEBS Lett.* **579**, 1945-1950.

Lee, S. L., Dickson, R. B. and Lin, C. Y. (2000). Activation of hepatocyte growth factor and urokinase/plasminogen activator by matriptase, an epithelial membrane serine protease. *J. Biol. Chem.* **275**, 36720-36725.

Leyvraz, C., Charles, R. P., Rubera, I., Guitard, M., Rotman, S., Breiden, B., Sandhoff, K. and Hummler, E. (2005). The epidermal barrier function is dependent on the serine protease CAP1/Prss8. *J. Cell Biol.* **170**, 487-496.

Lin, C. Y., Anders, J., Johnson, M. and Dickson, R. B. (1999). Purification and characterization of a complex containing matriptase and a Kunitz-type serine protease inhibitor from human milk. *J. Biol. Chem.* **274**, 18237-18242.

List, K., Haudenschild, C. C., Szabo, R., Chen, W., Wahl, S. M., Swaim, W., Engelholm, L. H., Behrendt, N. and Bugge, T. H. (2002). Matriptase/MT-SP1 is required for postnatal survival, epidermal barrier function, hair follicle development, and thymic homeostasis. *Oncogene* **21**, 3765-3779.

List, K., Szabo, R., Wertz, P. W., Segre, J., Haudenschild, C. C., Kim, S. Y. and Bugge, T. H. (2003). Loss of proteolytically processed filaggrin caused by epidermal deletion of Matriptase/MT-SP1. *J. Cell Biol.* **163**, 901-910.

List, K., Szabo, R., Molinolo, A., Sriuranpong, V., Redeye, V., Murdock, T., Burke, B., Nielsen, B. S., Gutkind, J. S. and Bugge, T. H. (2005). Deregulated matriptase causes ras-independent multistage carcinogenesis and promotes ras-mediated malignant transformation. *Genes Dev.* **19**, 1934-1950.

List, K., Bugge, T. H. and Szabo, R. (2006a). Matriptase: potent proteolysis on the cell surface. *Mol. Med.* **12**, 1-7.

List, K., Szabo, R., Molinolo, A., Nielsen, B. S. and Bugge, T. H. (2006b). Delineation of matriptase protein expression by enzymatic gene trapping suggests diverging roles in barrier function, hair formation, and squamous cell carcinogenesis. *Am. J. Pathol.* **168**, 1513-1525.

Lopez-Otin, C. and Bond, J. S. (2008). Proteases: multifunctional enzymes in life and disease. *J. Biol. Chem.* **283**, 30433-30437.

Marlor, C. W., Delaria, K. A., Davis, G., Muller, D. K., Greve, J. M. and Tamburini, P. P. (1997). Identification and cloning of human placental bikunin, a novel serine protease inhibitor containing two Kunitz domains. *J. Biol. Chem.* **272**, 12202-12208.

Mathias, J. R., Dodd, M. E., Walters, K. B., Rhodes, J., Kanki, J. P., Look, A. T. and Huttenlocher, A. (2007). Live imaging of chronic inflammation caused by mutation of zebrafish Hai1. *J. Cell Sci.* **120**, 3372-3383.

Mitchell, K. J., Pinson, K. I., Kelly, O. G., Brennan, J., Zupicich, J., Scherz, P., Leighton, P. A., Goodrich, L. V., Lu, X., Avery, B. J. et al. (2001). Functional analysis of secreted and transmembrane proteins critical to mouse development. *Nat. Genet.* **28**, 241-249.

Mizuno, K., Tanoue, Y., Okano, I., Harano, T., Takada, K. and Nakamura, T. (1994). Purification and characterization of hepatocyte growth factor (HGF)-converting enzyme: activation of pro-HGF. *Biochem. Biophys. Res. Commun.* **198**, 1161-1169.

Myerburg, M. M., Butterworth, M. B., McKenna, E. E., Peters, K. W., Frizzell, R. A., Kleyman, T. R. and Pilewski, J. M. (2006). Airway surface liquid volume regulates ENaC by altering the serine protease-protease inhibitor balance: a mechanism for sodium hyperabsorption in cystic fibrosis. *J. Biol. Chem.* **281**, 27942-27949.

Naldini, L., Tamagnone, L., Vigna, E., Sachs, M., Hartmann, G., Birchmeier, W., Daikuhara, Y., Tsubouchi, H., Blasi, F. and Comoglio, P. M. (1992). Extracellular proteolytic cleavage by urokinase is required for activation of hepatocyte growth factor/scatter factor. *EMBO J.* **11**, 4825-4833.

Netzel-Arnett, S., Currie, B. M., Szabo, R., Lin, C. Y., Chen, L. M., Chai, K. X., Antalis, T. M., Bugge, T. H. and List, K. (2006). Evidence for a matriptase-prostasin proteolytic cascade regulating terminal epidermal differentiation. *J. Biol. Chem.* **281**, 32941-32945.

Oberst, M. D., Singh, B., Ozdemirli, M., Dickson, R. B., Johnson, M. D. and Lin, C. Y. (2003). Characterization of matriptase expression in normal human tissues. *J. Histochem. Cytochem.* **51**, 1017-1025.

Page-McCaw, A., Ewald, A. J. and Werb, Z. (2007). Matrix metalloproteinases and the regulation of tissue remodelling. *Nat. Rev. Mol. Cell Biol.* **8**, 221-233.

Paoloni-Giacobino, A., Chen, H., Peitsch, M. C., Rossier, C. and Antonarakis, S. E. (1997). Cloning of the TMPRSS2 gene, which encodes a novel serine protease with transmembrane, LDLRA, and SRCR domains and maps to 21q22.3. *Genomics* **44**, 309-320.

Picard, N., Eladari, D., El Moghrabi, S., Planes, C., Bourgeois, S., Houillier, P., Wang, Q., Burnier, M., Deschenes, G., Knepper, M. A. et al. (2008). Defective ENaC processing and function in tissue kallikrein-deficient mice. *J. Biol. Chem.* **283**, 4602-4611.

Puente, X. S., Sanchez, L. M., Overall, C. M. and Lopez-Otin, C. (2003). Human and mouse proteases: a comparative genomic approach. *Nat. Rev. Genet.* **4**, 544-558.

Qin, L., Denda, K., Shimomura, T., Kawaguchi, T. and Kitamura, N. (1998). Functional characterization of Kunitz domains in hepatocyte growth factor activator inhibitor type 2. *FEBS Lett.* **436**, 111-114.

Quesada, V., Ordonez, G. R., Sanchez, L. M., Puente, X. S. and Lopez-Otin, C. (2009). The Degradome database: mammalian proteases and diseases of proteolysis. *Nucleic Acids Res.* **37**, D239-D243.
Rancourt, D. E., Tsuzuki, T. and Capecchi, M. R. (1995). Genetic interaction between hoxb-5 and hoxb-6 is revealed by nonallelic noncomplementation. *Genes Dev.* **9**, 108-122.
Rau, J. C., Beaulieu, L. M., Huntington, J. A. and Church, F. C. (2007). Serpins in thrombosis, hemostasis and fibrinolysis. *J. Thromb. Haemost.* **5** Suppl. 1, 102-115.
Rine, J. and Herskowitz, I. (1987). Four genes responsible for a position effect on expression from HML and HMR in Saccharomyces cerevisiae. *Genetics* **116**, 9-22.
Scudamore, C. L., Jepson, M. A., Hirst, B. H. and Miller, H. R. (1998). The rat mucosal mast cell chymase, RMCP-II, alters epithelial cell monolayer permeability in association with altered distribution of the tight junction proteins ZO-1 and occludin. *Eur. J. Cell Biol.* **75**, 321-330.
Shimomura, T., Kondo, J., Ochiai, M., Naka, D., Miyazawa, K., Morimoto, Y. and Kitamura, N. (1993). Activation of the zymogen of hepatocyte growth factor activator by thrombin. *J. Biol. Chem.* **268**, 22927-22932.
Szabo, R., Netzel-Arnett, S., Hobson, J. P., Antalis, T. M. and Bugge, T. H. (2005). Matriptase-3 is a novel phylogenetically preserved membrane-anchored serine protease with broad serpin reactivity. *Biochem. J.* **390**, 231-242.
Szabo, R., Molinolo, A., List, K. and Bugge, T. H. (2007). Matriptase inhibition by hepatocyte growth factor activator inhibitor-1 is essential for placental development. *Oncogene* **26**, 1546-1556.
Szabo, R., Hobson, J. P., List, K., Molinolo, A., Lin, C. Y. and Bugge, T. H. (2008). Potent inhibition and global co-localization implicate the transmembrane kunitz-type serine protease inhibitor hai-2 in the regulation of epithelial matriptase activity. *J. Biol. Chem.* **283**, 29495-29504.
Takano, N., Matusi, H. and Takahashi, T. (2004). Granzyme N, a novel granzyme, is expressed in spermatocytes and spermatids of the mouse testis. *Biol. Reprod.* **71**, 1785-1795.
Takeuchi, T., Harris, J. L., Huang, W., Yan, K. W., Coughlin, S. R. and Craik, C. S. (2000). Cellular localization of membrane-type serine protease 1 and identification of protease-activated receptor-2 and single-chain urokinase-type plasminogen activator as substrates. *J. Biol. Chem.* **275**, 26333-26342.
Vallet, V., Chraibi, A., Gaeggeler, H. P., Horisberger, J. D. and Rossier, B. C. (1997). An epithelial serine protease activates the amiloride-sensitive sodium channel. *Nature* **389**, 607-610.
Varkey, J. P., Jansma, P. L., Minniti, A. N. and Ward, S. (1993). The Caenorhabditis elegans spe-6 gene is required for major sperm protein assembly and shows second site non-complementation with an unlinked deficiency. *Genetics* **133**, 79-86.
Velasco, G., Cal, S., Quesada, V., Sanchez, L. M. and Lopez-Otin, C. (2002). Matriptase-2, a membrane-bound mosaic serine proteinase predominantly expressed in human liver and showing degrading activity against extracellular matrix proteins. *J. Biol. Chem.* **277**, 37637-37646.
Wallrapp, C., Hahnel, S., Muller-Pillasch, F., Burghardt, B., Iwamura, T., Ruthenburger, M., Lerch, M. M., Adler, G. and Gress, T. M. (2000). A novel transmembrane serine protease (TMPRSS3) overexpressed in pancreatic cancer. *Cancer Res.* **60**, 2602-2606.
Wang, M. H., Gonias, S. L., Skeel, A., Wolf, B. B., Yoshimura, T. and Leonard, E. J. (1994a). Proteolytic activation of single-chain precursor macrophage-stimulating protein by nerve growth factor-gamma and epidermal growth factor-binding protein, members of the kallikrein family. *J. Biol. Chem.* **269**, 13806-13810.
Wang, M. H., Yoshimura, T., Skeel, A. and Leonard, E. J. (1994b). Proteolytic conversion of single chain precursor macrophage-stimulating protein to a biologically active heterodimer by contact enzymes of the coagulation cascade. *J. Biol. Chem.* **269**, 3436-3440.
Wang, M. H., Skeel, A. and Leonard, E. J. (1996). Proteolytic cleavage and activation of pro-macrophage-stimulating protein by resident peritoneal macrophage membrane proteases. *J. Clin. Invest.* **97**, 720-727.